EXPERIMENT NO. 2

IMU CALIBRATION FOR SATELLITE NAVIGATION SYSTEMS

Submitted by:

Kush Jani

AEROSPACE AND OCEAN ENGINEERING DEPARTMENT

VIRGINIA POLYTECHNIC INSTITUTE AND STATE UNIVERSITY

BLACKSBURG, VIRGINIA

26 OCTOBER 2025

EXPERIMENT PERFORMED 13 OCTOBER 2025

LAB TEACHING ASSISTANT: NAGA NITISH CHAMALA

I. Abstract

This report contains an investigation into the calibration of inertial measurement units (IMUs) enabled through Virginia Tech's AOE Electronics Educational Center and Laboratory. The primary objective of this investigation was the characterization and correction of errors caused by bias, scale factor and axis misalignment for a 3-axis accelerometer and 3-axis gyroscope. This was done via the use of a 5-position static test which allowed for the isolation of the local gravitational field and provided known inputs for accelerometer calibration creating an overdetermined system of equations which could subsequently be solved for a correction matrix and bias vector. The gyroscope was also calibrated using both the zero-input data generated via the 5-position static test as well as three test cases using known angular velocities applied by a single-axis rate turntable to similarly overdetermine a system and create a correction matrix and bias vector for correction. The efficacy of these calibration procedures was verified and validated through the use of a multi-axis rate turntable which applied sinusoidal motion to the IMU and allowed for subsequent analysis to be performed and remaining bias for angular rate measured as well as the drift in the integrated angles reported by the IMU. The resulting successful calibration of the accelerometer and partially unsuccessful calibration of the gyroscope highlights the importance of the IMU for navigation and control as well as the merits/limitations present in the procedural methods and models behind these investigations.

IMU CALIBRATION FOR SATELLITE NAVIGATION SYSTEMS

Kush Jani[1]
Virginia Tech, Blacksburg, VA 24060

II. Introduction

The goals of this study are:

1. To calibrate an IMU's 3-axis accelerometer using a 5-position static test and the least squares method to determine the corresponding bias and correction matrices.
2. To calibrate an IMU's 3-axis gyroscope using a precision rate table to determine the corresponding bias and correction matrices.
3. To validate the efficacy of the systematic processes used in the calibration of the accelerometer and gyroscope by analyzing the performance of the IMU on multi-axis sinusoidal motion.

These goals were accomplished by utilizing a single-axis rate turntable as well as a Scorsby motion test turntable in order to subject the IMU to various known inertial inputs. The IMU and turntables are showcased in Fig. 1 and Fig. 2 respectively. The theoretical basis for this experiment is summarized as follows:

Inertial measurement units are foundational devices at the base of modern autonomous or semi-autonomous navigation systems used in large scale applications like satellite attitude control and unmanned aerial vehicle (UAV) and tactical missile guidance systems to more common uses cases in smartphones and robotics. IMU devices output high-frequency data on angular rates and linear accelerations which is then integrated over time through dead reckoning to determine system orientations and trajectories, especially in environments where external navigation aids like GPS are denied or unavailable. However, the capabilities of these devices are thus fundamentally limited by inherent sensor errors originating from manufacturing imperfections, specifically manifesting as biases (non-zero output under zero input), scale factor errors (incorrect output scaling), and axis misalignments (non-orthogonality of the sensing axes to external axes). Without correction, these deterministic errors lead to unbounded accumulation of drift due to the integrated nature of the dead reckoning process, resulting in unusable long-term navigation.

In order to avoid this fundamental constraint, correction on the sensor errors is done through modeling of sensor errors as a linear system that can be characterized and subsequently corrected. Specifically, the relationship between the raw sensor output and the true physical quantity can be modeled as a linear transformation where, in the case of a 3-axis accelerometer, the measured output vector U_a is related to the true acceleration vector a by the equation

$$U_a = B_a + K \cdot a + n_a \tag{1}$$

where B_a is the 3×1 bias vector, K is a 3×3 correction matrix with scale factors on its diagonal and cross-coupling coefficients as its off-diagonal terms, and n_a represents zero-mean random noise. Similarly, for the 3-axis gyro scope, a linear transformation is modeled such that the measured angular rate vector U_ω is related to the true angular rate vector ω by the equation

$$U_\omega = B_\omega + N \cdot \omega + n_\omega \tag{2}$$

where B_ω is the gyroscope bias vector and N is its corresponding correction matrix.

Through these models, the error terms can be determined by solving the overdetermined system of equations, which itself is created by subjecting the IMU to various known inputs and recording sensor outputs. This allows for the creation of a system of the form $U = G \times X$ where U is the matrix of known inputs, G is the matrix of corresponding sensor measurements, and X is the calibration matrix. The system can thus be solved via the least-squares method as shown by the equation

$$X = (G^T G)^{-1} G^T U \tag{3}$$

For this investigation, the known inertial inputs were static orientations in the local gravitational field and constant angular velocities, which were used to solve for the calibration matrices corresponding to the accelerometer and gyroscope respectively. These calibration matrices were subsequently used to correct the raw sensor data in real time to reduce angular drift with relatively complex sinusoidal motion.

[1] Undergraduate student, Aerospace & Ocean Engineering Department.

The remainder of this report is as follows: Section III describes the experimental setup, instrumentation, and methodology used for the investigation alongside a remark regarding the data acquisition code. Section IV presents the results of the investigation including the calibration matrices tabulated, graphical comparisons of raw versus uncalibrated data, and a brief discussion on the potential improvements to the investigation's methodology. Finally, Section V contains a discussion on the implications from the results of the investigation on guidance, navigation, and control (GN&C/GNC).

III. Apparatus and Techniques

A. Instrumentation

For this investigation, a Modulino Movement board as shown in Fig. 1 was used for the LSM6DSOX IMU sensor which integrates both a 3-axis accelerometer and a 3-axis gyroscope into one sensor. In order to apply precise known inertial inputs necessary for the calibration of the gyroscope, an Ideal Aerosmith 1270VS Single-Axis Rate Table (leftmost apparatus in Fig. 2) was used with angular rotation set to 3, 5, and 7 deg/s in either the clockwise or counterclockwise direction. During validation, an Ideal Aerosmith 1421 Scorsby Motion Test Table (rightmost apparatus in Fig. 2) was used to generate the multi-axis sinusoidal motion needed. For the calibration of the accelerometer, gyroscope, and validation on the Scorsby motion test turntable, a 3D printed test stand, as shown in Fig. 3, was placed atop the inactive single-axis rate turntable in order to orientate the IMU to various orthogonal axes with respect to the local gravitational field such that measurements were precise and the IMU remained secure whilst in motion. An Arduino UNO R4 WiFi board, as shown in Fig. 4, operated as a server during data transmission by transmitting sensor data read from the connected IMU to the client data acquisition system via a built-in Bluetooth Low Energy (BLE) module. The transmission is accomplished by preloaded C++ code which interacted with the IMU to read the raw sensor data and managed the transmission of the data. The data acquisition system itself is a laptop running the *dataAcquisitionCodeArduino.py* python script shown in Fig. 5, which would receive data sent out via Bluetooth from the Arduino.

B. Calibration and Experimental Technique

The experimental methodology for this investigation was separated into three distinct phases involving the calibration of the accelerometer, calibration of the gyroscope, and the validation of the calibration phases. In order to solve for the calibration matrix using the method from the theoretical background for this investigation as shown in Eq. 3 involved a central process of collecting raw sensor data under known inertial inputs and conditions to generate the measurement matrix G and input matrix U such that the system of equations becomes overdetermined, allowing for the solution of the least-squares problem to be found.

For the first phase involving the calibration of the accelerometer, the errors for the accelerometer were characterized by isolating the local gravitational vector along each of the sensor's axes. This involved securely mounting the IMU into the aforementioned 3D printed test stand such that the sensor is oriented directly along an axis. For instance, by having the IMU placed parallel to the ground, the $+Z$ axis points directly upwards perpendicular to the ground such that the known acceleration vector can be set to $[0,0,+1]^T g$ where $g \approx 9.81\ m/s^2$. Repeating for the remaining orientations (excluding $-Z$ due to the incompatibility of the test stand to accommodate the IMU orientated directly downwards) results in known vectors of $[0,+1,0]^T g$, $[0,-1,0]^T g$, $[+1,0,0]^T g$, $[-1,0,0]^T g$ for +Y, -Y, +X, -X respectively. Data for each orientation was acquired for 10 seconds resulting in 38 entries per orientation which were averaged to provide an average value for each recorded category of Raw Accel in X, Raw Accel in Y, Raw Accel in Z, Raw Gyro in X, Raw Gyro in Y, Raw Gyro in Z, Cal Accel in X, Cal Accel in Y, Cal Accel in Z, Cal Gyro in X, Cal Gyro in Y, Cal Gyro in Z, Roll Angle, Pitch Angle, and Yaw Angle. For the calibration of the accelerometer, only the raw accelerations in X, Y, & Z were utilized in the G matrix. The G is formed such that row corresponds to an orientation and contains a leading '1' for the bias term followed by the averaged raw acceleration outputs A_x, A_y, A_z. The U matrix is thus the known inertial input vectors organized in a manner as to correspond to the order of the averaged raw acceleration outputs in G. These matrices are then used to solve Eq. 3, as done via the code shown in Fig. 6, before inserting the calculated bias and calibration matricies into the *dataAcquisitionCodeArduino.py* script to ensure subsequent analysis utilizes a calibrated accelerometer.

For the second phase involving the calibration of the gyroscope, the errors are characterized in a similar manner as in the first phase, albeit through the use of a known angular velocity applied by the Ideal Aerosmith single-axis rate turntable rather than the local gravitational field. This turntable was initially set to rotate at a

constant velocity of 3 $°/s$ clockwise to generate a known velocity vector of $[0,0,-3]^T$ $°/s$ by having the IMU mounted inside of the test stand orientated with the $+Z$ upwards perpendicular to the ground so that the Z-axis aligned with the table's axis of rotation. The turntable was subsequently set to rotate at constant velocities of 5 $°/s$ clockwise and 7 $°/s$ counterclockwise where the IMU was reorientated to have the $+Y$ and $+X$ axis aligned with the table's axis of rotation respectively, resulting in correspondingly known velocity vectors of $[+7,0,0]^T$ $°/s$ and $[0,-5,0]^T$ $°/s$. The data for each of these trials was acquired over the course of 30 seconds causing 113 entries in each of the aforementioned recorded categories to be output into spreadsheets before being averaged as done in the first phase. Unlike the first phase, the raw gyroscopic motion in X, Y, & Z were used to create the G matrix along with the use of gyroscopic entries recorded in the first phase providing data for raw sensor reading of gyroscopic motion with zero angular velocities due to the first phase involving only static testing. This results in an 8×4 matrix for G and an 8×3 matrix for U due to the additional five entries from the first phase zero-rate input data and the additional column of ones for the bias in G. The calculation of the calibration matrix is done by the code shown in Fig. 6 once more before being inserted along with the bias matrix into the *dataAcquisitionCodeArduino.py*.

During the validation phase, the fully calibrated IMU is mounted onto the Ideal Aerosmith multi-axis rate turntable to produce sinusoidal multi-axis motion, with data acquisition taking place over 30 seconds during which roll, pitch, and yaw angles are plotted in real time.

C. Data Acquisition Scripting

The *dataAcquisitionCodeArduino.py* python script operates as the primary tool for data acquisition and real time plotting by connecting with the Arduino server and receiving a stream of IMU data packets which are recorded and output into Excel spreadsheets for further manual processing to be performed. Specifically, during the first phase of the experiment, the script is utilized solely for acquiring and recording the data where identity matrices were used for scaling and zero vectors were used for bias. Following this first phase, the recorded data from the script was inserted into the separate script shown in Fig. 6, which performed the core calculation by being a direct implementation in Python of the least squares normal equation shown by Eq. 3. This allowed for a calibration matrix and bias vector to be generated and inserted into the *dataAcquisitionCodeArduino.py* script to allow for partial calibration prior to calibration of the gyroscope. Following the gyroscope calibration in the second phase, the same process for calculating the calibration matrix and bias vector for insertion into *dataAcquisitionCodeArduino.py* was repeated to ensure a fully calibrated IMU with correction enabled during the third phase. The compilation of the G and U matrices was performed manually from the manually time-averaged data extracted from the spreadsheets output by the *dataAcquisitionCodeArduino.py* script.

IV. Results and Discussion

A. Accelerometer Calibration and Validation

The 5-position static test was performed, and corresponding data was processed in accordance with the methodology described in Section III. The time-averaged raw accelerometer data for the five static positions were used to construct the matrix G_{accel} given by

$$G_{accel} = \begin{bmatrix} 1 & 1.0097 & -0.0230 & -0.0015 \\ 1 & -1.0017 & -0.0386 & -0.0111 \\ 1 & 0.0169 & 0.9721 & -0.0252 \\ 1 & 0.0065 & -1.0194 & 0.0578 \\ 1 & 0.0145 & -0.0059 & 1.0236 \end{bmatrix}$$

The corresponding matrix of known inertial input accelerations U_{accel} is thus given by

$$U_{accel} = \begin{bmatrix} 1 & 0 & 0 \\ -1 & 0 & 0 \\ 0 & 1 & 0 \\ 0 & -1 & 0 \\ 0 & 0 & 1 \end{bmatrix}$$

Solving the least-squares problem shown in Eq. 3 results in X_{accel}, a 4×3 calibration matrix, which was decomposed into the bias vector and the correction matrix B_{accel} and K_{accel} respectively, given as

$$B_{accel} = \begin{bmatrix} -0.0079 \\ 0.0275 \\ -0.0036 \end{bmatrix} g \quad , \quad K_{accel} = \begin{bmatrix} 0.9943 & -0.0055 & -0.0066 \\ -0.0077 & 1.0034 & -0.0212 \\ -0.0051 & 0.0408 & 0.9803 \end{bmatrix}$$

During the validation testing performed via the Scorsby motion test turntable trial, these matrices were utilized and resulted in a plot being generated as shown in Fig. 7 via spreadsheet graphing. From the plot, it becomes evident that accelerometer was effectively calibrated such that the acceleration vector magnitude became much closer to the actual 1g of gravitational force being applied during static testing. Analyzing the bias term, where the largest error of 2.75% is recorded on the Y-axis, it is apparent that the initial errors were small but notable. Furthermore, the scale factors shown on the diagonal of the correction matrix are very close to one with the largest deviation being 1.97% on the Z-axis. Furthermore, the off-diagonal elements are relatively small, representing a small misalignment of the axes with the largest term of 0.0408 corresponding to a misalignment angle of $\sin^{-1} 0.0408 = 2.34°$ between the Y and Z axes.

B. Gyroscope Calibration and Validation

Similar to the accelerometer calibration, the gyroscope calibration utilized the raw gyroscopic data for the X, Y, and Z axes from the 5 static tests performed as zero-input data alongside 3 non-zero input data cases extracted from the three single-axis rotation cases conducted on the single-axis rate turntable. The time-averaged raw gyroscope data from these eight measurements were used to construct the matrix G_{gyro} given by

$$G_{gyro} = \begin{bmatrix} 1 & 0.1814 & 0.2933 & -0.8884 \\ 1 & 0.1662 & 0.2984 & -0.4764 \\ 1 & 0.0825 & 0.2804 & 0.2408 \\ 1 & 0.1780 & 0.2797 & -1.5835 \\ 1 & 0.1797 & 0.2831 & 0.3018 \\ 1 & 0.1820 & 0.1815 & -3.6376 \\ 1 & 6.2212 & 0.2038 & 0.3128 \\ 1 & 0.1619 & -4.1956 & -0.8463 \end{bmatrix}$$

The corresponding matrix of known inertial input angular velocities U_{gyro} is thus given by

$$U_{gyro} = \begin{bmatrix} 0 & 0 & 0 \\ 0 & 0 & 0 \\ 0 & 0 & 0 \\ 0 & 0 & 0 \\ 0 & 0 & 0 \\ 0 & 0 & -3 \\ 7 & 0 & 0 \\ 0 & -5 & 0 \end{bmatrix}$$

Note that the first five rows are zero rows corresponding to the first five rows of the G_{gyro} matrix which utilized the zero-input raw gyroscopic data garnered from the five static position tests conducted. Solving the least-squares problem shown in Eq. 3 results in X_{gyro}, a 4×3 calibration matrix, which was decomposed into the bias vector and the correction matrix B_{gyro} and K_{gyro} respectively, given as

$$B_{gyro} = \begin{bmatrix} -0.1718 \\ -0.33280 \\ 0.2712 \end{bmatrix} °/s \quad , \quad K_{gyro} = \begin{bmatrix} 1.1519 & 0.0005 & 0.0143 \\ 0.0182 & 1.1186 & -0.0282 \\ -0.0766 & -0.0822 & 0.7301 \end{bmatrix}$$

The gyroscope inherently exhibits a greater error than the accelerometer as shown by the bias vector B_{gyro} with a notable constant drift rate of $-0.3328°/s$ which, if uncorrected, would rapidly accumulate through the integration based dead reckoning process and cause a large error in the pitch angle calculations. Furthermore, the scale factor errors seen on the diagonal terms of K_{gyro} are also substantial with deviations from one ranging from -26.9% to 15.2% compared to the maximum deviation of 1.97% seen in the accelerometer. This demonstrates that the raw gyroscope inherently underreports the true rate of rotation in the Z axis while overreporting the rate of rotation in the X and Y axes. The off-diagonal terms remain relatively small, however, representing a small misalignment of the axes and cross-axes sensitivities.

The effectiveness of applying these corrections is shown via the plot in Fig. 8 and Fig. 9, which contain the "Gyroscope Calibration Validation Angular Rates" plot and "Gyroscope Calibration Validation Integrated Angles" respectively. From the plot contained in Fig. 8, the calibrated rates shown by dashed lines are clearly centered about the zero-degree line more effectively than the raw gyroscope data which indicated that the bias has successfully been corrected for and mitigated. However, the success of the calibration was only partially validated as the plot contained in Fig. 9 shows significant drift particularly in

the roll and pitch even following correction. However, it is apparent that the drift in yaw is significantly improved as the calibrated yaw integrated angle data demonstrated an apparent center about the zero-degree line as expected, especially in comparison to the raw yaw integrated angle data. Through analysis of the trendlines created, as given by the equations

$$\text{Cal Roll (X):} \quad y = -0.7053\,x - 3.9833 \tag{4}$$

$$\text{Cal Pitch (Y):} \quad y = -0.7385\,x + 4.1758 \tag{5}$$

$$\text{Cal Yaw (Z):} \quad y = 0.1905\,x - 5.4231 \tag{6}$$

From these equations, it is apparent that the calibrated yaw drift rate is indeed relatively small at $0.19\ °/s$ while the drift of roll and pitch post correction remains at $0.7\ °/s$. Furthermore, the amplitude of the integrated angles are approximately 18 to 20 degrees peak-to-peak for the Roll and Yaw whereas the Pitch amplitude is larger at around 25 degrees peak-to-peak. The expected amplitudes should be 17 to 20 degrees due to the one axis being set to 8.5 degrees while the other two axes were set to 10 degrees in the settings for the multi-axis rate turntable. This implies a potential cross-axis sensitivity or scale factor issue. However, the physical motion profile of the Scorsby table remains visible in the plots regardless of the partially unsuccessful calibration since the X and Z rates are roughly in phase while the Y rate is out of phase as expected.

C. Discussion on Potential for Improvements

While the calibration resulted in significant improvements to the IMU's performance in the accelerometer and some minor improvements to the gyroscope's angular rates bias, the validation revealed several limitations inherent to the procedure and model used. The most notable of these limitations is the residual drift show in Eq. 4 through Eq. 6 which remained ever following the correction for static bias. This indicates that a linear model may be insufficient in capturing the full spectrum of sensor errors due to the use of a constant bias and single scale factor matrix. The primary unmodeled error is likely the instability in the bias where the bias itself may drift. Since the period between static testing and validation was large due to the intermediate calculations and gyroscope calibration performed, a drift may have been reintroduced. Monitoring the drift over a period of time may result in polynomial fit being performed to model the bias and scale factors in a more accurate manner.

V. Conclusion

This investigation was partially successful in calibration of a 3-axis accelerometer and 3-axis gyroscope by fully correcting the minor bias present in the accelerometer as well as partially correcting the integrated angles and angular rate of the gyroscope. The following conclusions can be garnered from this investigation:

1. The 5-position test and least-squares method was greatly successful in calibrating the accelerometer as the resulting bias vector and correction matrix was capable of reducing mean error in the measured gravity vector magnitude by over 90% while improving the stability of the measurement significantly as shown via Fig. 7.
2. The gyroscope was found to have intrinsically large errors in axis misalignment and scale factors with deviations over 20% for scale factors. The methodology used for calibration of the gyroscope proved to be somewhat effective in improving the bias for the angular rates measured by the IMU but failed in mitigating the drift for both the pitch roll to a significant degree as shown in Fig. 9.

From the results of this investigation, the experimental methodology was proven to be effective in the calibration technique for the accelerometer and somewhat ineffective for the gyroscope as the potential for unmodeled errors and drift in the bias allowed for drift to remain post-correction in the calibrated IMU.

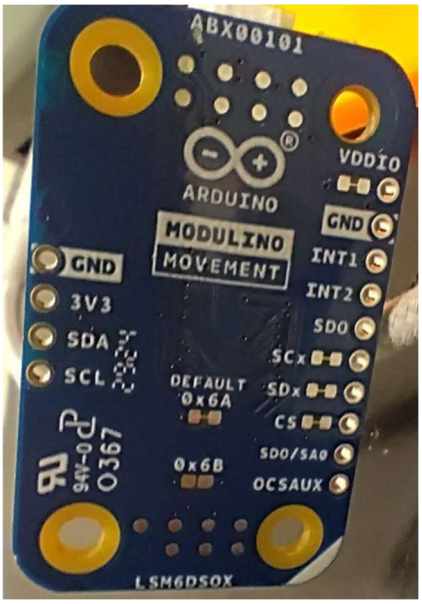

Fig. 1. Arduino Modulino Movement.

Single-axis Rate Table (Top)
Multi-axis Rate Table (Right

Fig. 2. Single Axis & Multi-Axis Rate Table. Adapted from Davoudi (2025).

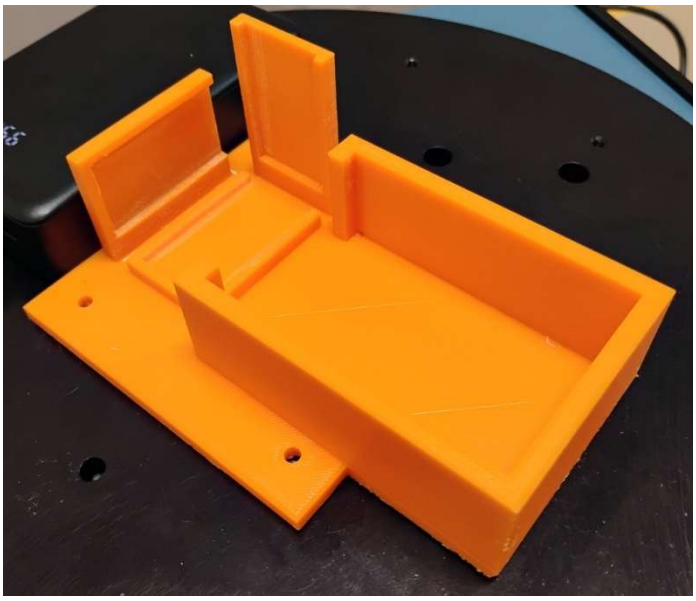

Fig. 3. 3D Printed Test Stand.

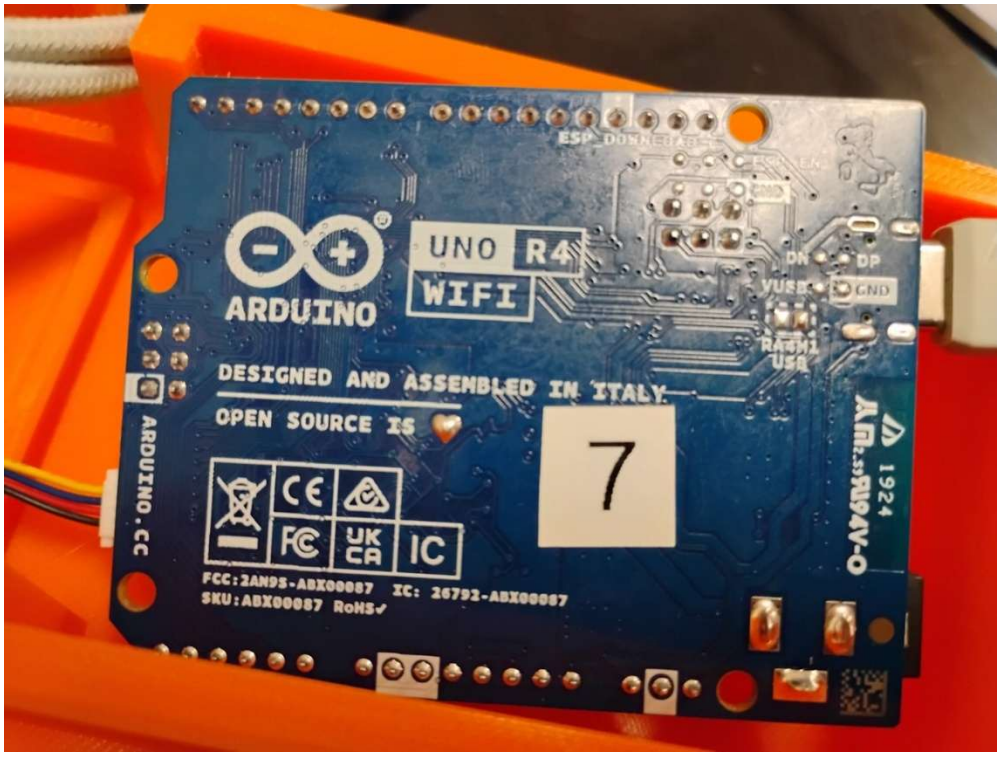

Fig. 4. Arduino UNO R4 WiFi Board.

Fig. 5. dataAcquisitionCodeArduino.py

```python
import numpy as np

g = 9.81

G = np.array([[1, 10.05,  0.15, -0.20], [1, -9.55,  0.13, -0.22], [1,  0.21, 10.11, -0.18],
    [1,  0.25, -9.50, -0.25], [1,  0.23,  0.18,  9.95], [1,  0.19,  0.21, -9.70]])

U = np.array([[ g,  0,  0], [-g,  0,  0], [ 0,  g,  0], [ 0, -g,  0], [ 0,  0,  g], [ 0,  0,
     -g]])

GT = G.transpose()
GTG = np.dot(GT, G)
GTG_inverse = np.linalg.inv(GTG)
GTU = np.dot(GT, U)
X = np.dot(GTG_inverse, GTU)

print(X)
```

Fig. 6. Python Script to Implement Eq. 3.

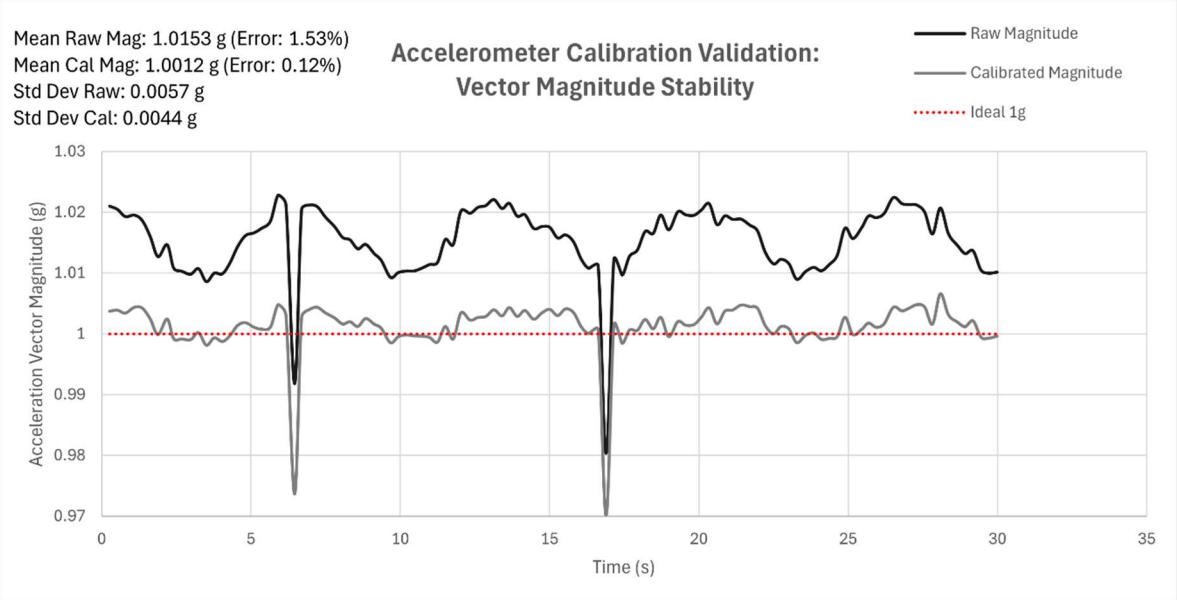

Fig. 7. Accelerometer Calibration Validation: Vector Magnitude Stability.

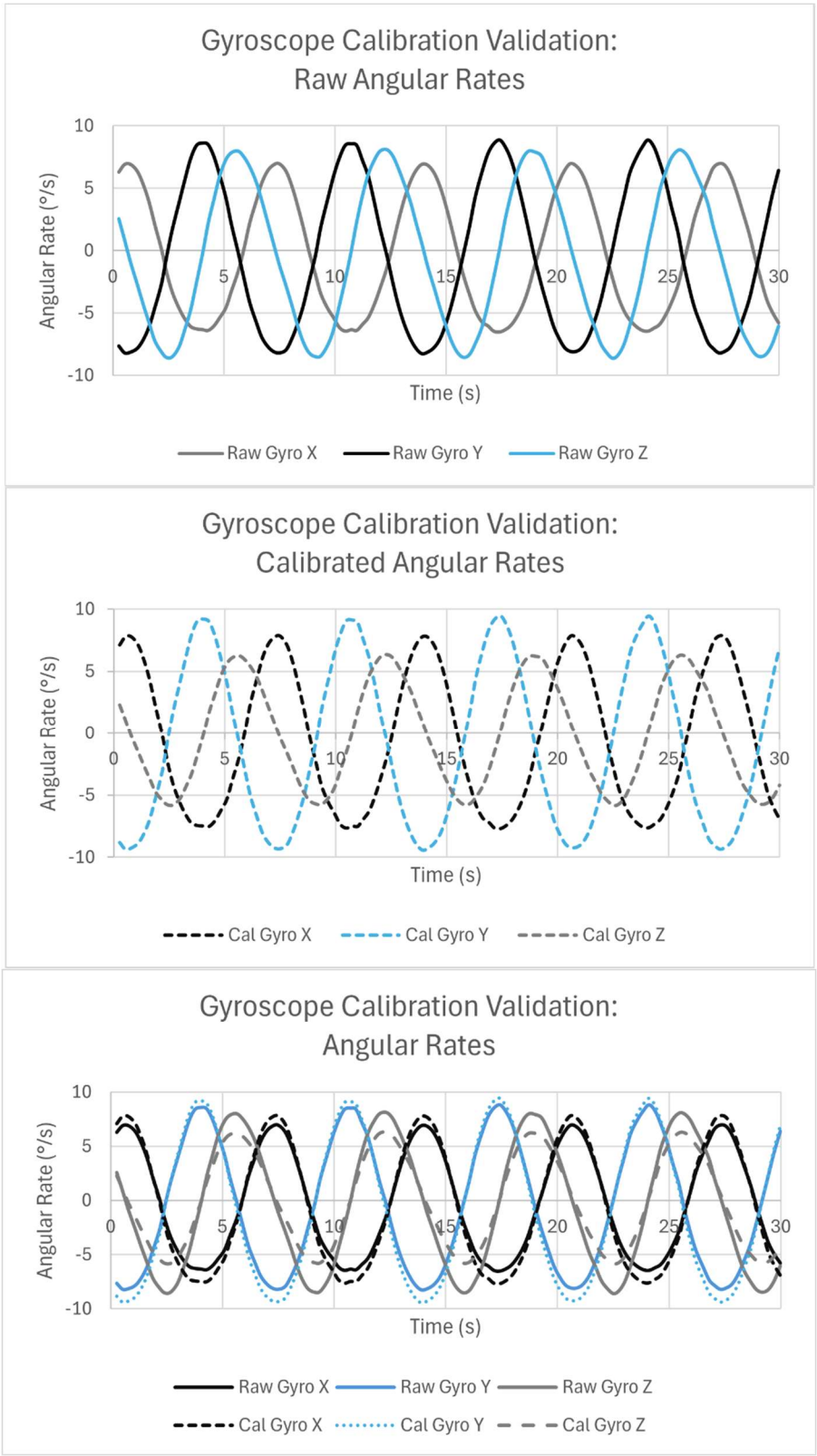

Fig. 8. Gyroscope Calibration Validation: Angular Rates.

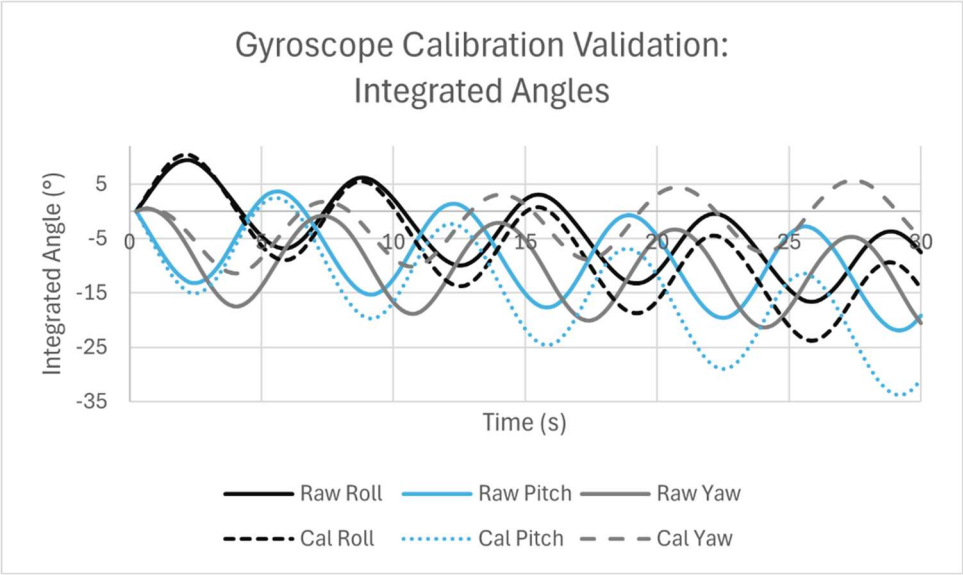

Fig. 9. Gyroscope Calibration Validation: Integrated Angles.

REFERENCES

B. Davoudi, "AOE 4105 — IMU Calibration for Satellite Navigation Systems," Virginia Polytechnic Institute and State University, [Oct. 1, 2025]. Lab Manual.

Appendix A

A. Uncertainty Analysis

Uncertainties in derived quantities were calculated using the root-sum-square (RSS) method and reported with 20:1 odds such that a 95% confidence interval is had resulting in a 95% probability that the true value of any such measurement lies within the range defined by the value $\pm$ its uncertainty.

To obtain the uncertainty in for variables dependent on several measured variables, the uncertainties are propagated using the equation

$$\delta(R) = \sqrt{\left(\frac{\partial R}{\partial a}\delta(a)\right)^2 + \left(\frac{\partial R}{\partial b}\delta(b)\right)^2 + \left(\frac{\partial R}{\partial c}\delta(c)\right)^2 + \cdots} \tag{7}$$

where the variables a,b,c… are the variables that R depends on and were measured. The most notable sources of uncertainty in this experiment are the precision of the known inertial inputs used for calibration. Namely, the gravitational field was approximated to have a strength of 9.81 meters per second squared. Furthermore, a potential uncertainty may have been the result of sensor noise which was mitigated by time-averaging the data, as well as misalignment during insertion into the test stand. As a result, uncertainty for the purpose of this experiment was disregarded due to the small scale of the errors that would have been accumulated and lack of non-qualitatively measured uncertainties.